Food Chemistry: X 24 (2024) 101913

Contents lists available at ScienceDirect

Food Chemistry: X

journal homepage: www.sciencedirect.com/journal/food-chemistry-x

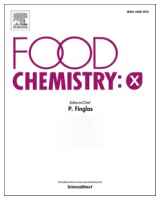

Study on the effects of pre-slaughter transport stress on water holding capacity of pork: Insights from oxidation, structure, function, and degradation properties of protein

Chao Ma [a], Jian Zhang [b], Ruyu Zhang [a], Lei Zhou [a], Laixue Ni [c], Wangang Zhang [a,*]

[a] State Key Laboratory of Meat Quality Control and Cultured Meat Development, Ministry of Education China, Jiangsu Collaborative Innovation Center of Meat Production and Processing, Quality and Safety Control, College of Food Science and Technology, Nanjing Agricultural University, Nanjing 210095, China
[b] College of Food Science and Light Industry, Nanjing Tech University, Nanjing 211816, China
[c] Linyi Jinluo Win Ray Food Co., Ltd., Linyi 276036, China

ARTICLE INFO

Keywords:
Pre-slaughter transport stress
Protein oxidation
Protein structure
Protein degradation
Microstructure
Water holding capacity

ABSTRACT

This work systematically investigated the effects of pre-slaughter transport stress on pork water holding capacity (WHC) during aging from the perspectives of oxidation, structure, function, and degradation properties of protein. Pigs were randomly divided into three-hour transport (Transport-induced stress, T group) and three-hour transport followed by three-hour resting (Control, TR group). Results demonstrated that T treatment markedly declined pork WHC. Compared with TR group, T group presented increased oxidation levels. Meanwhile, T treatment exacerbated the shift of protein secondary structure from α-helix to random coil and protein unfolding levels. The decreased solubility, thermal stability, and degraded levels of proteins were also observed in T group. Additionally, muscle contractions of T group were more severe than TR group. This study supported that pre-slaughter transport stress altered physicochemical properties and structures of postmortem muscle proteins, which reduced pork WHC via impairing the interactions between protein and water molecules and changing the muscle fiber structure.

1. Introduction

Water holding capacity (WHC), defined as the ability of fresh meat to maintain intrinsic moisture, is a critical quality attribute of fresh meat. It not only influences the edible quality and nutritional value of postmortem pork but also directly affects the economic value of pork industry (Szmanko, Lesiow, & Gorecka, 2021). The WHC of fresh meat is affected by many factors including genotype (Salas & Mingala, 2017), pre-slaughter handling (e.g., transport and resting) (Xing, Gao, Tume, Zhou, & Xu, 2019), aging method (Chen, Zhou, & Zhang, 2015), and others. Among these, pre-slaughter handling is considered as the most direct and common factor affecting WHC of fresh meat (Faucitano, 2018). Investigations from Zhou, Shen, Liu, Wang, and Shen (2019) and Ma, Zhang, Zhou, and Feng (2023) have suggested that slaughtering immediately after transport could reduce pork WHC and increase the incidence of abnormal meat, while resting for two or three hours could allowed pigs to well recover from transport stress, thus remarkably reducing above adverse effects. Likewise, other scholars have also demonstrated that meat quality especially WHC could be pronouncedly decreased when pigs subjected to transport or acute exercise were not performed to pre-slaughter three-hour resting (Young, Bertram, & Oksbjerg, 2009). Despite these observations, the cause behind these phenomena remains unclear and needs to be further studied.

It is currently known that pre-slaughter stress can lead to a faster rate of pH drop by accelerating postmortem muscle glycolysis, which is more likely to induce protein denaturation and in turn alter the functional properties of muscle proteins (Lesiów & Xiong, 2013). In meat, reduced meat WHC has been demonstrated to be related to increased levels of myofibrillar protein (MP) denaturation and decreased protein solubility (Bowker & Zhuang, 2015). Additionally, now a growing stream of reports shows that unreasonable pre-slaughter handling can lead to the overproduction of reactive oxygen species (ROS) and reactive nitrogen species (RNS) in postmortem muscle (Ma, Zhang, Zhang, & Du, 2023; Xing et al., 2019). Protein oxidation reactions triggered by these reactive

* Corresponding author at: 205 National Center of Meat Quality and Safety Control, College of Food Science and Technology, Nanjing Agricultural University, Nanjing, Jiangsu 210095, China.
E-mail address: wangang.zhang@njau.edu.cn (W. Zhang).

https://doi.org/10.1016/j.fochx.2024.101913
Received 7 August 2024; Received in revised form 10 October 2024; Accepted 19 October 2024
Available online 21 October 2024

free radicals can induce amino acid side-chain modifications, loss of reactive sulfhydryl (SH) groups, raise of protein hydrophobicity, and generation of protein crosslinks (Zhang, Xiao, & Ahn, 2013). Thus, it is reasonable to assume that multiple properties of postmortem muscle proteins during aging may be changed in response to pre-slaughter stress levels in pigs. Furthermore, these alterations may further lead to substantial variability in meat WHC via altering the spatial arrangement pattern of protein structure and impairing degraded levels of critical cytoskeleton proteins, limiting the swelling of myofibrils, and reducing the myofilament space (Estevez, Ventanas, Heinonen, & Puolanne, 2011). In recent years, oxidative damage and structural changes in meat proteins, especially MPs, have received considerable interest in terms of their potential role and significance in meat WHC (Chen et al., 2015; Li et al., 2023; Wang, Wang, Li, & Zhang, 2019). However, for a long time, researchers have mainly focused on studying the changes in the metabolic state of early postmortem muscle caused by various pre-slaughter stressors and in turn the effects on postmortem pork quality (Xing et al., 2019). Systematic investigation on pre-slaughter transport stress-induced variations in oxidation, structure, function, and degradation of proteins as well as their impacts on muscle fiber structure and thus pork WHC during postmortem aging are largely lacking.

Thus, this study aimed to provide a systematic understanding of the changes in oxidation levels, protein structural, functional, and degraded properties, as well as WHC in pork during postmortem aging in response to pre-slaughter transport stress. Antioxidant enzyme activities and ROS levels at 1 and 24 h postmortem were detected to assess the muscle oxidative stability in the early postmortem. Carbonyl and SH contents were measured to identify the differences in oxidative levels during postmortem aging. Circular dichroism (CD) spectrum, bromophenol blue (BPB) binding amount, intrinsic fluorescence intensity, particle size, solubility, and thermal stability were used to evaluate changes in structure and functional characteristics of meat proteins. Immunoblotting was used to detect the μ-calpain autolysis and degradation levels of caspase-3 as well as key cytoskeleton proteins, including desmin, troponin T (TnT), and filamin C. Additionally, drip loss, cooking loss, and low-field nuclear magnetic resonance (LF-NMR) were measured to identify the differences in WHC. The changes in the tissue structure of pork *longissimus thoracis* (LT) muscle during postmortem aging were also examined to further explain the physical and chemical variations in pork from a macroscale insight.

2. Materials and methods

2.1. Materials and chemicals

Bicinchoninic acid (BCA) kit, phosphate-buffered saline (PBS), 5,5'-Dithiobis-(2-nitrobenzoic acid) (DTNB), and precast gels were purchased from Solarbio Science &Technology Co., Ltd. (Beijing, China). BPB was purchased from Yuanye Biotechnology Co., Ltd. (Shanghai, China). Biuret protein concentration, carbonyl content, and antioxidant enzyme activity assay kits as well as 2,7-dichlorofluorescein diacetate were purchased from Jiancheng Bioengineering Co., Ltd. (Nanjing, China). Caspase-3 activity assay kit was purchased from Beyotime Biotechnology Co., Ltd. (Shanghai, China). All other reagents were of analytical grade.

2.2. Experimental design and sampling preparation

A total of 16 castrated crossed pigs (Duroc × Landrace × Yorkshire) with an age of 6 months (110 ± 10 kg) were randomly selected from a commercial farm (Zhengda Pig Industry Co., Ltd., Suqian, China). Then, the pigs were randomly assigned to two groups (n = 8): three-hour transport without resting (Transport-induced stress, T group) and three-hour transport followed by three-hour resting (Control, TR group). The transport vehicle was driven on a flat road (60 km/h) without stops. During transport, the average ambient temperature was about 30 °C. The pigs were slaughtered by severance of the jugular veins after electrical stunning at a commercial slaughter factory (Sushi Meat Products Co., Ltd., Huai'an, China) according to the Chinese national slaughtering standards (GB/T 19479-2019). At 1 h postmortem, the left and right LT muscles (6 × 6 × 12 cm^3) were excised from both sides of the carcasses, and aged at 4 °C. The right LT muscle was taken at 1 h, 24 h (aging 0 d), 96 h (aging 3 d), and 168 h (aging 6 d) postmortem, quickly frozen in liquid nitrogen, and then stored at −80 °C for the determination of biochemical indicators. The left LT muscle was taken at the corresponding aging point for the evaluation of WHC and water status as well as the observation of tissue structure. Previously, we have demonstrated that the stress levels of pigs in the T group were significantly higher than those in the TR group based on the plasma stress indicators (Ma, Zhang, Zhang, & Du, 2023), and thus the obtained samples were reliable for the subsequent analysis considering the aim of this investigation.

2.3. WHC and water status

The cooking loss and drip loss were detected to assess pork WHC during postmortem aging. For the cooking loss, the samples were trimmed into regular pieces (2 × 3 × 5 cm^3) along the myofibril direction and weighed as M1. The electrothermal digital probe was inserted into the center of the samples, and then the packed samples were immersed in a water bath at 72 °C until the center temperature reached 70 °C. Then, the samples were cooled with running water and weighed again as M2. The cooking loss was obtained by the equation: cooking loss (%) = (M1 − M2)/M1 × 100 %. For the drip loss, the meat samples were trimmed into regular pieces (1 × 1 × 3 cm^3) along the myofibril direction and weighed as M3. Then, the samples were suspended in a light-tight sealed incubator and stored at 4 °C. Finally, the samples were weighed again as M4 at each aging time point. The drip loss was obtained by the equation: drip loss (%) = (M3 − M4)/M3 × 100 %.

LF-NMR was used to assess the water status referring to Chen et al. (2015). The meat samples were trimmed into 1 × 1 × 2 cm^3 along the myofibril direction and then placed in a cylindrical NMR tube. Measurements were conducted using the CPMG sequence. The parameter settings were as follows: sampling was repeated eight times, the repetition interval was 4000 ms, the number of echoes was 3000, and the relaxation time of 0.01–3000 ms was fitted. Finally, the data was inverted using MultiExpInv analysis software (NMI20-040H-I, Newman Analytical Instrument co., Ltd., Su Zhou, China).

2.4. Antioxidant enzyme activities and ROS levels

The LT muscle (0.1 g) was added to 0.9 mL of pre-chilled 0.01 M PBS and homogenized at 5000 rpm for 20 s (4 °C) (Ultra Turrox T25 Basic, IKA, Germany). Then, the homogenate was centrifuged at 3000g for 10 min at 4 °C. The Glutathione peroxidase (GSH-Px), superoxide dismutase (SOD), and catalase (CAT) activities of supernatant were determined by using commercial kits, and the ROS levels in LT muscle were detected with 2,7-dichlorofluorescein diacetate (Liao, Zhang, Li, Xing, & Gao, 2022).

2.5. Carbonyl content

The carbonyl content of pork LT muscle was assessed by a commercial kit. The minced meat sample (0.1 g) was added to 0.9 mL of pre-cooled reagent I and homogenized at 10,000 rpm for 20 s (4 °C). The homogenate was centrifuged at 2500g for 10 min (4 °C). Afterward, 50 μL of reagent II and 450 μL of supernatant were fully mixed, placed at room temperature for 10 min, and then centrifuged at 11,000g for 10 min. Then, the obtained supernatant was collected to detect carbonyl content according to the procedure of instructions (Zhang et al., 2024).

2.6. MPs extraction

The extraction of MPs followed the method of Yin, Zhou, Pereira, Zhang, and Zhang (2020). All operations are carried out at 4 °C. Briefly, 4 g meat samples were added to 16 mL of pre-cooled buffer A (0.1 M KCl, 10 mM K_2HPO_4, 1 mM EGTA, and 2 mM $MgCl_2$, pH 7.0) and homogenized at 10,000 rpm (30 s × 3) with a 15 s interval. The homogenate was centrifuged at 2000*g* for 20 min, and the pellets were collected. After the above procedures were repeated three times, the precipitates were again homogenized with 16 mL buffer B (0.1 M KCl) at 10,000 rpm (30 s × 2) with 15 s intervals and then the mixture was filtered with a single gauze. After the mixture was centrifuged at 2000*g* for 20 min, the precipitates were collected to repeat the above process twice. Then, the obtained pellet MP was dissolved in pre-cooled buffer C (0.6 M KCl and 10 mM KH_2PO_4, pH 6.0) for further analysis. The MP concentration was measured by a BCA kit.

2.7. SH content

Total and free SH contents were evaluated by referring to the procedures of Yin et al. (2020). The 0.5 mL homogenate with a protein concentration of 1 mg/mL was mixed with 5 mL of buffer solution (10 M EDTA, 20 mM Tris−HCl, and 8 M urea, pH 6.0). The mixture was incubated at 37 °C for 30 min in the dark after adding 0.1 mL of 10 mM DTNB. Then, the samples were centrifuged at 12,000*g* for 15 min. The absorbance value of the supernatant was detected at 412 nm (SpectraMax M2e, Molecular Devices, Sunnyvale, CA, USA). The total SH contents were obtained using an extinction coefficient of 13,600 M^{-1} cm^{-1}. Free SH content was assessed using the same procedures as above, but except mixing with buffer solution.

2.8. MP structure

2.8.1. Secondary structure

CD spectrometer (J-1500, Jasco, Japan) was performed to detect MP secondary structure. MP solutions (0.2 mg/mL) were transferred to a quartz cell (0.1 cm width) at 22 °C and scanned from 200 to 260 nm with 100 nm/min. Finally, the CD spectrum was analyzed by the software's program.

2.8.2. Surface hydrophobicity and intrinsic fluorescence intensity

The surface hydrophobicity of MP was evaluated by the method of Chen et al. (2015). The 40 μL of 1 mg/mL BPB were well mixed with 2 mL of 2 mg/mL MP solutions. The buffer C (0.6 M KCl and 10 mM KH_2PO_4, pH 6.0) was used as a blank. All samples were placed at 4 °C for 10 min, followed by centrifugation at 10,000*g* for 15 min (4 °C). Then, the absorbance value of supernatant was detected at 595 nm. The amount of bound BPB was expressed as the surface hydrophobicity and obtained by the equation: BPB (μg) = 40 × (OD blank − OD sample)/OD blank.

The intrinsic fluorescence intensity of MP was evaluated by using a Jasco fluorescence spectrophotometer (RF-5301, Jasco, Tokyo, Japan). The MPs solution (1 mg/mL) was scanned at an excitation wavelength of 280 nm and an emission wavelength between 300 and 400 nm. The excitation and emission slit widths were fixed at 5.0 nm.

2.8.3. Particle size

The average particle size of MP solution (0.2 mg/mL) was detected by a Zetasizer Nano-ZS 90 instrument (Malvern Instruments LTD, Malvern, UK). The dispersant was set as water with a refractive index of 1.330, and the equilibration time was established at 120 s.

2.9. Protein solubility

The protein solubility was analyzed by referring to the procedures of Chen et al. (2015). The meat sample (1 g) was added to 20 mL of pre-chilled 1.1 M potassium iodide dissolved in 0.1 M potassium phosphate buffer (pH 7.2) and homogenized at 2500 rpm (20 s × 3) with a 20 s interval under ice bath conditions. Then, the homogenate was extracted overnight with shaking (4 °C), followed by centrifugation at 2000*g* for 15 min (4 °C). The protein concentration of supernatant was measured by a Biuret kit and expressed as total protein solubility (S1). The sarcoplasmic protein solubility (S2) was detected using the same procedure as above, except for the buffer (10 mL of pre-chilled 25 mM potassium phosphate buffer, pH 7.2). MP solubility (S3) was obtained by the equation: S3 (mg/g) = S1 − S2.

2.10. Thermal stability

Differential scanning calorimetry (DSC) (DSC8000, PerkinElmer, Massachusetts, USA) was employed to measure protein thermal stability. The samples of T ($n = 8$) and TR groups (n = 8) were weighed with the same weight, and then randomly combined into 4 pairs in each group. Briefly, the meat samples (20 ± 1 mg) were transferred into an aluminum pan and sealed with a capper. Thermal scan was conducted over the rising temperature range of 20–100 °C at a scan speed of 10 °C/min. A sealed empty aluminum pan was employed as the control. The maximum transition temperature was obtained by analyzing the DSC thermogram.

2.11. Protein degradation

Briefly, 0.5 g of minced samples at 3 d of aging were added to 4.5 mL of buffer (100 mM HEPES, 0.1 mM neocuproine, 1 mM EDTA, and 1 % SDS, pH 7.8) to homogenize at 10,000 rpm (3 × 15 s, 4 °C). Then the homogenate was centrifuged at 10,000*g* for 15 min (4 °C). The protein concentration of the supernatant was determined using a BCA kit, subsequently adjusted to 6 mg/mL with HENS buffer, and then mixed with loading buffer (pH 6.8) at 1:1 and boiled at 95 °C for 5 min. The 30 micrograms of protein were used to detect the degradation levels of proteolytic enzymes (μ-calpain and caspase-3) and critical cytoskeleton proteins (desmin, TnT, and filamin C) through an electrophoresis system and transfer printing operations. The primary antibody of μ-calpain (MA3–940, Thermo Fisher, USA), caspase-3 (ab4051, Abcam, Cambridge), desmin (ab8976, Abcam, UK), troponin T (T6277, Sigma-Aldrich, Germany), filamin C (ab180941, Abcam, UK) and β-tubulin (A19654, Abclonal, China) were diluted with TBST solution (1:5000, 1:1000, 1:1000, 1:1000, 1:10,000, and 1:1000), respectively. The other operations were the same as our previous research (Ma, Zhang, Zhou, & Feng, 2023; Du, Ma, Wang, Hao and Zhang, 2023). In addition, caspase-3 activity was measured using a commercial kit.

2.12. Microstructure

Briefly, muscle tissue (0.5 × 0.5 × 1 cm^3) was cut along the direction of the muscle fibers and placed in 4 % paraformaldehyde (pH 7.0) for overnight fixation. Then, the muscles were gradually dehydrated in anhydrous ethanol (75 %, 85 %, and 90 % for 2 h; 95 % for 1 h; and 100 % for 30 min) and embedded in paraffin. Afterward, samples were cut into 7 mm sections in a direction perpendicular to the myofibrils and processed by the hematoxylin and eosin (H&E) staining solution. Finally, the muscle fiber structure was observed under an optical microscope (Eclipse E100, Nikon, Japan) at a magnification of 200×, and the muscle fiber gap in at least three fields of view from three tissue sections per replicate was measured using Image J software (NIH, Bethesda, MD).

In addition, the samples (3 × 5× 0.5 mm^3) for scanning electron microscope (SEM) with an accelerating voltage of 5 kV (SU-8010, Hitachi, Tokyo, Japan) were cut from the surface of pork muscles and fixed for 48 h at 4 °C with 2.5 % glutaraldehyde in 0.1 M PBS (pH 7.3). The muscle slice was next transferred to 0.1 M phosphate butter (pH 7.3) in 1 % osmium tetroxide for 5 h. After washing three times with PBS (pH

7.3), slices were dipped in incremental concentrations of ethanol (from 50 % to 100 %, each for 30 min) to dehydrate and then placed in acetone for further dehydration. Then, the samples were washed three times with tert-butyl alcohol and frozen at −20 °C. After freeze-dried and plated with gold, the ultrastructure of the muscle fibers was observed under SEM at a magnification of 200× and 500×.

2.13. Statistical analysis

The data were analyzed by the SPSS 22 (IBM Corporation, Armonk, NY) and the results were shown as mean ± standard deviation. A univariate model with Fisher's Least Significant Difference test was conducted at the 5 % level to analyze the significance of the treatment group, aging time, and their interaction. In addition, the *t*-test was conducted to analyze the differences in indicators related to protein degradation.

3. Results and discussion

3.1. WHC and water status

Drip loss denotes the leakage of free water and immobile water of muscle tissue under conditions characterized by gravity alone without the application of any external force. Cooking loss, including water evaporation, fat melting, and soluble protein loss, are strongly associated with muscle juiciness and quality. Pre-slaughter handling method (PM) and aging time (AT) significantly affected the drip loss and cooking loss of pork ($p < 0.05$, Table S1), while their interaction had no significant effect ($p > 0.05$). Additionally, the drip loss throughout the aging period and cooking loss at 3 and 6 d in the T group were significantly higher relative to the TR group ($p < 0.05$, Fig. 1 A and B), suggesting that pre-slaughter transport stress notably impaired pork WHC during postmortem aging. The poorer WHC of T group detected in this study is consistent with previous reports (Young et al., 2009; Zhou et al., 2019). This phenomenon could be explained by increased calcium (Ca^{2+}) levels and resulting intense muscle contraction induced by pre-slaughter transport stress (Xing et al., 2019), which in turn possibly lowed the pH of postmortem muscle and changed moisture distribution characteristics.

The LF-NMR technique is commonly conducted to reflect moisture migration and distribution in fresh meat and meat product. Three components including T_{2b}, T_{21}, and T_{22} of all samples were obtained (Fig. 1C). T_{2b} is bound water (1–10 ms), and its water state is hardly affected even by severe mechanical external forces. T_{21} (10–100 ms)

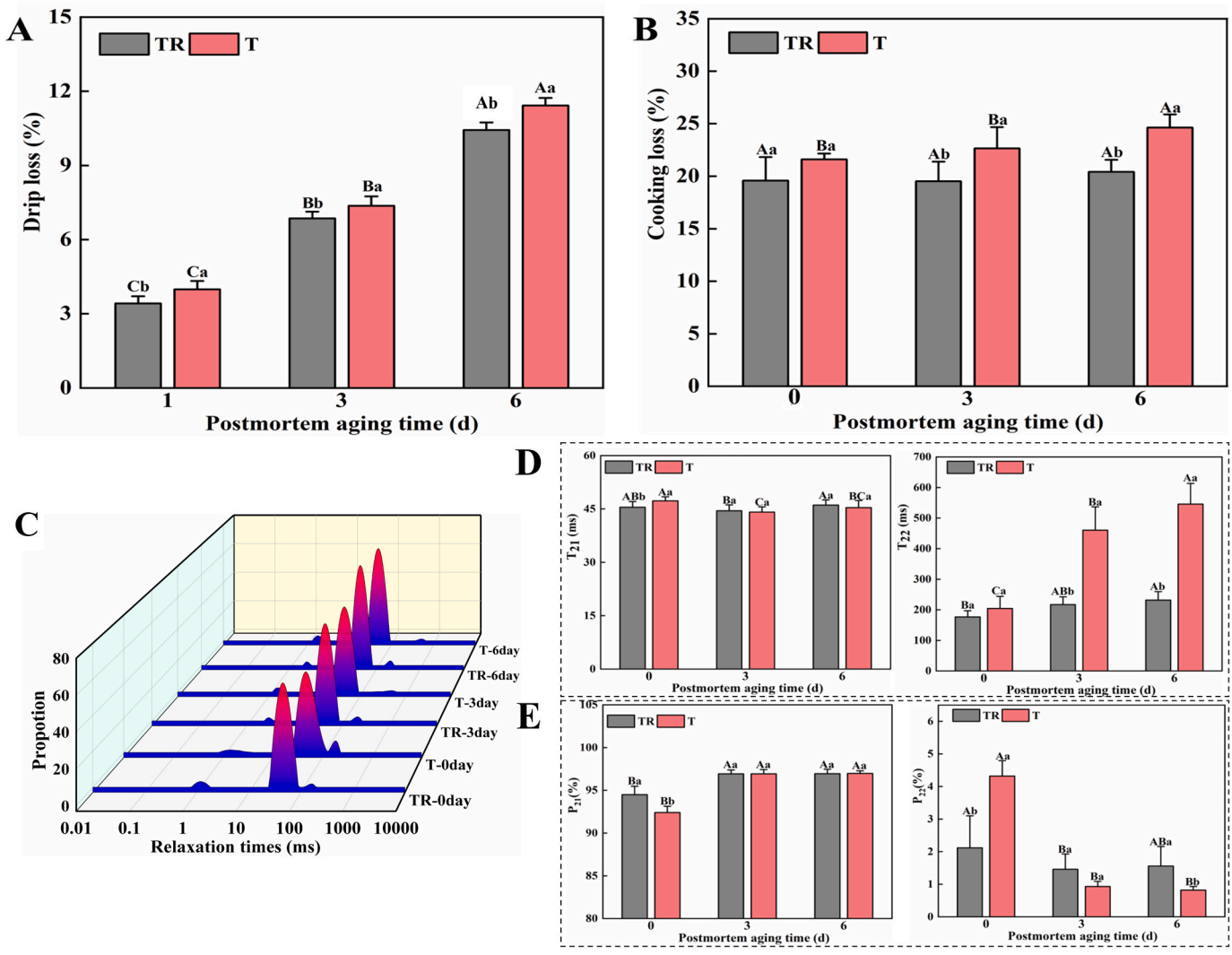

Fig. 1. Effect of pre-slaughter transport stress on the water holding capacity and water distribution of pork during postmortem aging, (A) drip loss, (B) cooking loss, (C) LF-NMR relaxation time spectra, (D) T_{21} and T_{22} relaxation times, and (E) P_{21} and P_{22}. Different letters (A-C) indicate a significant difference among aging time points at the same treatment ($p < 0.05$); Different letters (a, b) indicate a significant difference between two treatments at the same aging time ($p < 0.05$). TR: three-hour transport followed by three-hour resting treatment; T: three-hour transport treatment.

represents immobilized water in protein-dense myofibrillar network, which is susceptible to changes in protein structure and charge. T_{22} (100–1000 ms) means the free water loosely distributed among muscle fibers. Correspondingly, P_{21} and P_{22} represent the peak areas of the two water types of T_{21} and T_{22}, respectively. As shown in Table S1, PM, AT, and their interaction significantly affected T_{22} and P_{21}, meanwhile, AT and its interaction with PM significantly affected T_{21} and P_{22} ($p < 0.05$). In addition, the T_{21} at 0 d and T_{22} at 3 and 6 d in the T group were significantly longer than in the TR group (Fig. 1D, $p < 0.05$), indicating that T group had higher water mobility during postmortem aging. Based on the observation of Fig. 1E, T group at 0 d presented a significantly lower P_{21} and a significantly higher P_{22} ($p < 0.05$) as compared to TR group. This result shows that the immobilized water in the T group migrated and transformed into free water that easily separated from the myofibrils. In line with Xing et al. (2016), who stated that pre-slaughter transport stress could weaken the binding of protein to water molecules, thereby contributing to a decreased P_{21} and an increased P_{22} of broiler breast meat. However, P_{22} in the T group was observed a significant decrease at 6 d relative to the TR group ($p < 0.05$). This could be attributed to worse WHC of T group, in which free water had been largely lost from muscle fibers during the aging process. In summary, these outcomes reveal that transport-induced stress remarkably increased water mobility, induced water migration, and ultimately led to deteriorated pork WHC during postmortem aging observed in the T group (Fig. 1A and B).

3.2. Oxidation levels

As shown in Fig. 2A, B, and C, compared with the TR group, the GSH-Px, SOD, and CAT activities of T group were relatively higher at 1 h postmortem, but the GSH-Px and SOD activities were relatively lower at 24 h postmortem ($p < 0.05$). As previously reported, muscles from stress-sensitive animals exhibited enhanced antioxidant enzyme activity that could serve as an adaptive defense mechanism for the organism (Shelepov, Tihonov, Gorlov, & Poznyakovskiy, 2015). Similarly, Liao et al. (2022) reported that pre-slaughter transport stress could activate the body's antioxidant enzyme defense system via improving the activities of GSH-Px, SOD, and Cu-Zn SOD in broiler skeletal muscle. However, the decreased activities of GSH-Px and SOD at 24 h postmortem in the T group could be attributed to rapidly reduced pH and high carcass temperature induced by pre-slaughter transport stress (Ma, Zhang, Zhou, & Feng, 2023), which might induce severe denaturation of GSH-Px and SOD and thus inhibit their activities (Carvalho et al., 2017). When the homeostasis of the endogenous antioxidant enzyme system was destroyed, ROS would be excessively produced, which could result in oxidative stress damage in postmortem muscle and thus deteriorate meat quality (Liao et al., 2022). Supportively, in the current study, it was found from Fig. 2D that ROS levels in the T group were markedly higher than those in the TR group at 1 and 24 h postmortem ($p < 0.05$).

Free amino acids (e.g., lysine and cysteine) of muscle proteins are extremely sensitive to an oxidative environment and easily oxidized to carbonyl groups as well as disulfide bonds, which in turn can induce the disruption of protein conformation, the formation of protein cross-linkage, and the increase of muscle shrinkage (Zhang et al., 2013). Thus, carbonyl and SH contents are widely used to reflect the oxidation levels of muscle proteins. As shown in Table S1, PM and AT significantly affected carbonyl content ($p < 0.05$), while their interaction showed no significant effect ($p > 0.05$). Besides, the carbonyl content of T group at 3

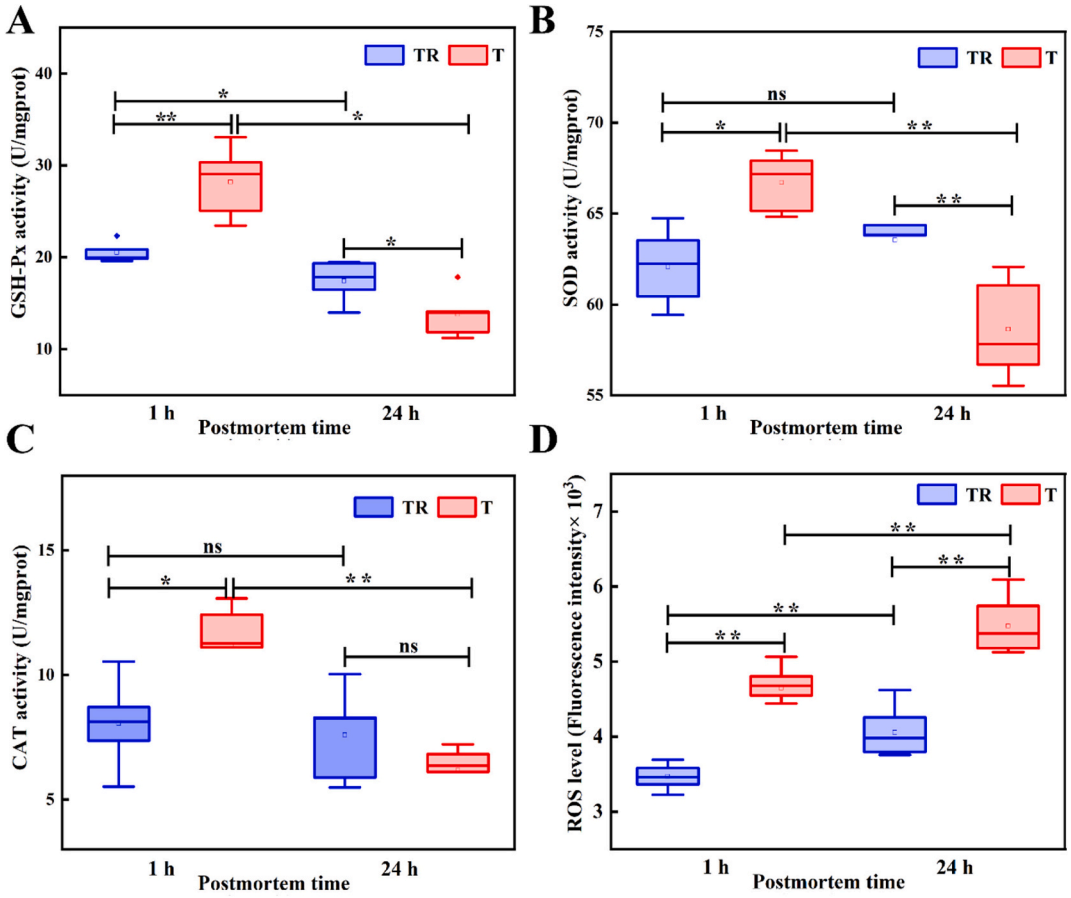

Fig. 2. Effects of pre-slaughter transport stress on the antioxidant enzyme activities and ROS levels in postmortem muscles, (A) GSH-Px, (B) SOD, (C) CAT, and (D) ROS levels. "*" indicate a significant difference at $p < 0.05$, "**" indicate a significant difference at $p < 0.01$. TR: three-hour transport followed by three-hour resting treatment; T: three-hour transport treatment.

and 6 d was significantly higher relative to the TR group ($p < 0.05$, Fig. 3A). This result suggests that the samples of T group were more susceptible to oxidation in the later stages of aging. One possible explanation is that the decreased antioxidant enzymes caused their inability to scavenge excess production of reactive free radicals in response to pre-slaughter stress, which then induced severe oxidative chain reactions in postmortem muscle (Carvalho et al., 2017). In addition, PM, AT, and their interaction significantly affected total and free SH contents ($p < 0.05$, Table S1). It can be observed in Fig. 3B that the total SH content of T group presented a significant reduction during the whole aging relative to the TR group ($p < 0.05$). For free SH, a noticeable decrease in the T group was also observed at 3 and 6 d ($p < 0.05$, Fig. 3C). According to the previous study, the varying degrees of reduction in total and free SH groups were mainly ascribed to active radicals-mediated protein oxidation modification, that is, the oxidation of SH groups to disulfide bonds and other oxidizing species, indicating increased protein oxidation levels and changes in protein structures (Jiang et al., 2022). Likewise, Cheng et al. (2022) recently reported that pre-slaughter heat stress exacerbated the degree of oxidative damage and structural destruction of duck meat proteins, causing serious negative impact on the quality attributes and nutritional value of duck meat.

3.3. MP structure

3.3.1. Secondary structure

The representative CD spectrums are shown in Fig. 4A, and it can be observed that CD spectrums exhibited two distinct peaks at 208 and 222 nm, demonstrating that α-helix was the main secondary structure in MP (Cao & Xiong, 2015). The factors of the PM, AT, and their interaction apparently influenced the ratio of α-helix and random coil, meanwhile, PM and AT significantly affected the ratio of β-sheet (Table S1, $p < 0.05$). The ratio of α-helix in the two groups presented a significant downward trend as the aging time increased ($p < 0.05$, Fig. 4B). In agreement with Jiang et al. (2022), who also demonstrated that α-helix ratio of pork proteins exhibited a decreasing trend during aging and mainly attributed it to the disruption of hydrogen bonds as well as the formation of protein aggregations. Moreover, at 0 and 6 d, the T group had a lower α-helix ratio and a higher random coil ratio relative to the TR group ($p < 0.05$). At 0 and 3 d, the T group presented a higher β-sheet ratio compared with the TR group ($p < 0.05$). Regarding the β-turn ratio, no significant change was found during postmortem aging ($p > 0.05$). Studies have elucidated that α-helix was a regularly ordered structure and considered to maintain the stability of protein conformation mainly through hydrogen bonds between carbonyl (C═O) and amino groups (—NH_2), while the increased β-sheet and random coil structures are responsible for the loose and open protein structure (Du et al., 2021). Thus, the current outcomes suggest that transport-induced stress caused the disruption of hydrogen bonds, which facilitated the shift of protein secondary structure from α-helix to β-sheet and random coil, implying the loosening of the protein structure and decreasing stability.

3.3.2. Tertiary structure

The BPB is similar to a fluorescent probe that can bind to the hydrophobic sites of protein, so the amount of bound BPB is widely used to assess the protein surface hydrophobicity and characterize the degree of change in the protein tertiary structure (Chelh, Gatellier, & Sante-Lhoutellier, 2006). Table S1 shows that PM and AT significantly affected protein surface hydrophobicity ($p < 0.05$), while their interaction showed no significant effect ($p > 0.05$). Besides, as shown in Fig. 4C, the T group at 3 and 6 d presented a higher protein surface hydrophobicity relative to the TR group ($p < 0.05$). This result indicates that after pre-slaughter transport stress, the hydrophobic groups buried inside the protein molecules of postmortem pork were easily exposed on the surface of protein during aging. Previous research has indicated that change in the intrinsic conformation unfolding of protein molecules is commonly accompanied by increased oxidative modification levels (Kang et al., 2016). Yin, Xing, and Zhang (2023) also showed that the surface hydrophobicity of beef MP increased following treatment with 1 mM hydrogen peroxide, implying that oxidative modification induced the unfolding of beef MP.

Additionally, tryptophan is the major source of intrinsic fluorescence in proteins and its residues are highly susceptible to changes in the internal microenvironment of proteins. Thus, the fluorescence intensity (FI) of intrinsic tryptophan was also used to assess the change of MP tertiary structure. As depicted in Fig. 4D, the FI in the two groups presented a decreasing trend with the aging time prolonged ($p < 0.05$). Besides, the FI at 0 and 3 d was dramatically lower in the T group relative to the TR group ($p < 0.05$). Tryptophan residues located in the hydrophobic environment inside the protein have a higher FI, but protein unfolding can cause tryptophan residues to be exposed to the hydrophilic environment producing a lower FI (Cao & Xiong, 2015). Accordingly, it could be known that transport-induced stress was prone to induce protein unfolding, thus causing a lower FI. Furthermore, the intermolecular interactions could also be strengthened with the exposure of the active region within the protein and thus induce the protein to re-aggregate to yield more hydrophobic molecules, which might further induce intrinsic fluorescence intensity quenching. In summary, the above results suggest that pre-slaughter transport stress increased the level of protein unfolding of pork during postmortem aging and consequently promoted the exposure of buried hydrophobic regions to

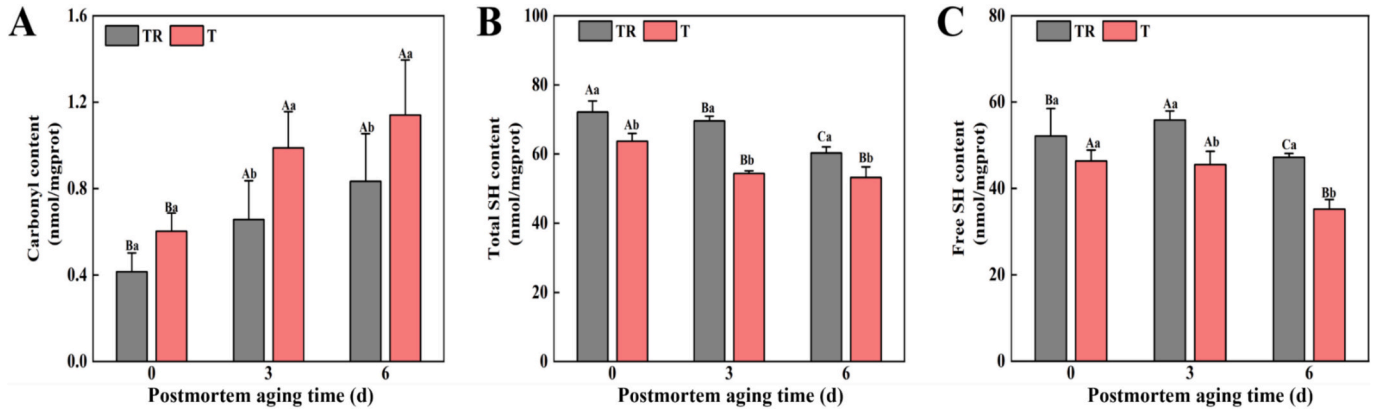

Fig. 3. Effects of pre-slaughter transport stress on the oxidation levels of pork during postmortem aging, (A) carbonyl content, (B) total SH content, and (C) free SH content. Different letters (A–C) indicate a significant difference among aging time points at the same treatment ($p < 0.05$); Different letters (a, b) indicate a significant difference between two treatments at the same aging time ($p < 0.05$). TR: three-hour transport followed by three-hour resting treatment; T: three-hour transport treatment.

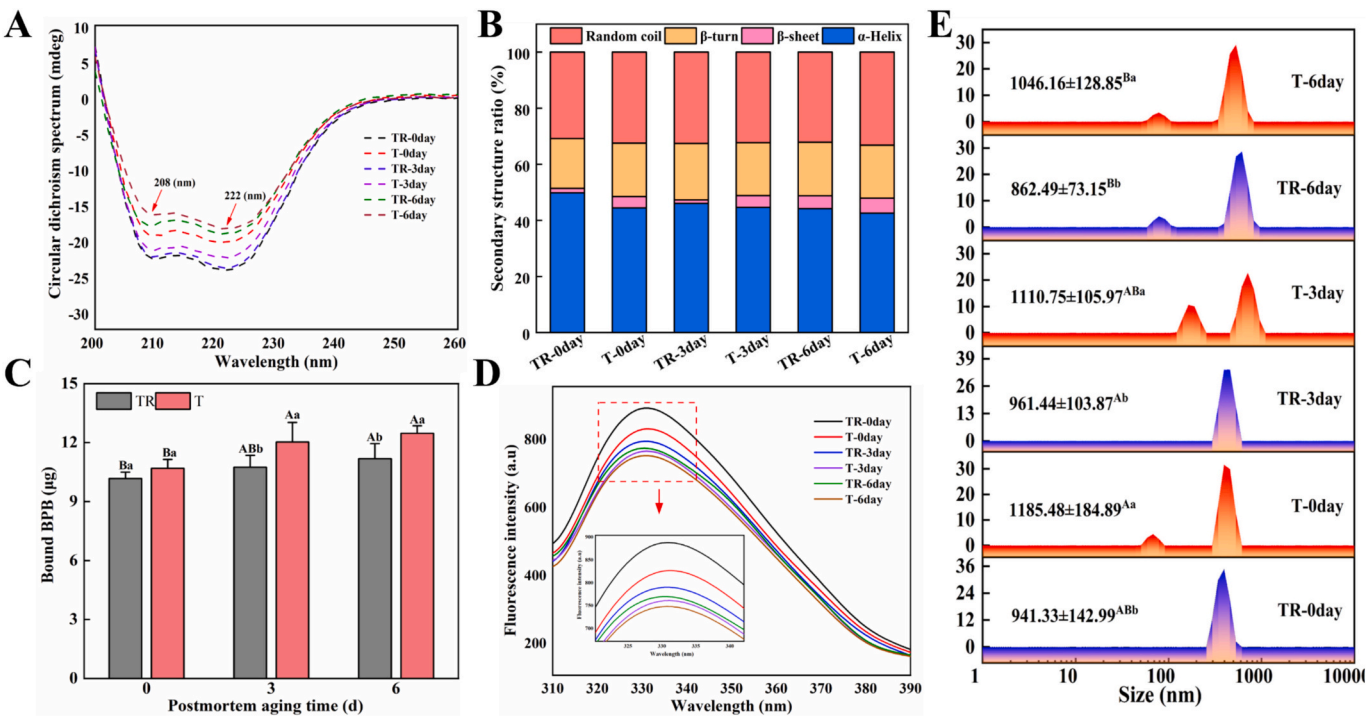

Fig. 4. Effects of pre-slaughter transport stress on the structure of pork MPs during postmortem aging, (A) CD spectra, (B) secondary structure ratio, (C) the amount of bound BPB, (D) intrinsic fluorescence spectra, and (E) particle size distribution spectra and average particle size. Different letters (A–C) indicate a significant difference among aging time points at the same treatment ($p < 0.05$); Different letters (a, b) indicate a significant difference between two treatments at the same aging time ($p < 0.05$). TR: three-hour transport followed by three-hour resting treatment; T: three-hour transport treatment.

the protein surface, impairing the binding capacity of protein and water molecules.

3.3.3. Particle size

Particle size is widely used to quantitatively evaluate the aggregation behavior of proteins and monitor the changes in protein structure (Cao et al., 2018). Fig. 4E depicts the particle size distribution spectrums of MP solution. The samples of T group presented a typical bimodal characteristic and a broader distribution range than those in the TR group, indicating that the MP solution of T group was not uniformly distributed and unstable. As Table S1 shows, PM and AT apparently influenced the average particle size of MP solution ($p < 0.05$), while their interaction showed no significant effect ($p > 0.05$). In addition, the average particle size in the T group was pronouncedly larger relative to the TR group at each aging time point ($p < 0.05$), suggesting that transport-induced stress accelerated the intermolecular cross-linking of proteins via inducing the formation of carbonyl cross-linked compound and disulfide bonds, as reflected by increased carbonyl group and decreased SH contents (Fig. 3). Meanwhile, the increase in average particle size could also be attributed to myosin filament unfolding and in turn the exposure of hydrophobic groups within proteins, implying the formation of protein aggregation and the destruction of hydrogen bonds (Promeyrat et al., 2010).

3.4. Functional properties of protein

3.4.1. Protein solubility

Protein solubility can reflect the degree of protein denaturation and aggregation and has a critical influence on the functional properties of protein (Qiu et al., 2022). As shown in Table S1, the PM and AT notably influenced the solubility of total protein, sarcoplasmic protein, and MP ($p < 0.05$), however, their interaction had no significant effect on their solubility ($p > 0.05$). For total protein solubility, the T group was remarkably lower during the whole aging relative to the TR group ($p < 0.05$, Fig. 5A). For MP solubility, the T group at 0 and 6 d was dramatically lower relative to the TR group ($p < 0.05$). As for the sarcoplasmic protein, the T group was dramatically lower than the TR group at 3 and 6 d ($p < 0.05$). Similar to our findings, Xing et al. (2016) previously reported that the solubility of MP and sarcoplasmic protein from broilers that experienced pre-slaughter transport stress was notably decreased. And the varying reductions in protein solubility of stress-induced samples were mainly associated with protein denaturation as a result of a rapidly reduced pH. Furthermore, Li, Wang, Kong, Shi, and Xia (2019) demonstrated that denatured proteins could further trigger the cross-linking of proteins to form aggregates with high molecular weight (> 200 kDa), which might further decrease protein solubility.

3.4.2. Thermal stability

As depicted in the DSC thermogram (Fig. 5B), three typical endothermic transition peaks were observed. The corresponding temperature of three transition peaks represents the maximum denaturation temperatures (T_{max}, °C) of myosin (T_{max1}), sarcoplasmic protein and collagen (T_{max2}), and actin (T_{max3}), respectively. It has been reported that the T_{max} could well reflect protein conformational integrity and protein denaturation levels. Table S1 shows that PM and AT obviously affected the T_{max1}, while PM, AT, and their interaction notably influenced the T_{max2} ($p < 0.05$). In terms of myosin (T_{max1}), the T group was dramatically decreased at 0 and 6 d relative to the TR group ($p < 0.05$, Fig. 5C). For sarcoplasmic protein and collagen (T_{max2}), the T group was dramatically reduced at 0 and 3 d than in the TR group ($p < 0.05$). Regarding actin (T_{max3}), the most thermostable protein in muscles, no noticeable difference was observed between the two groups during postmortem aging ($p > 0.05$). Similarly, Xing et al. (2016) indicated that the T_{max1} and T_{max2} in breast meat from broilers subjected to transport stress were significantly reduced implying the loss of structural and functional stability of myosin and sarcoplasmic proteins. The stability of the protein conformation is maintained by a variety of covalent and non-

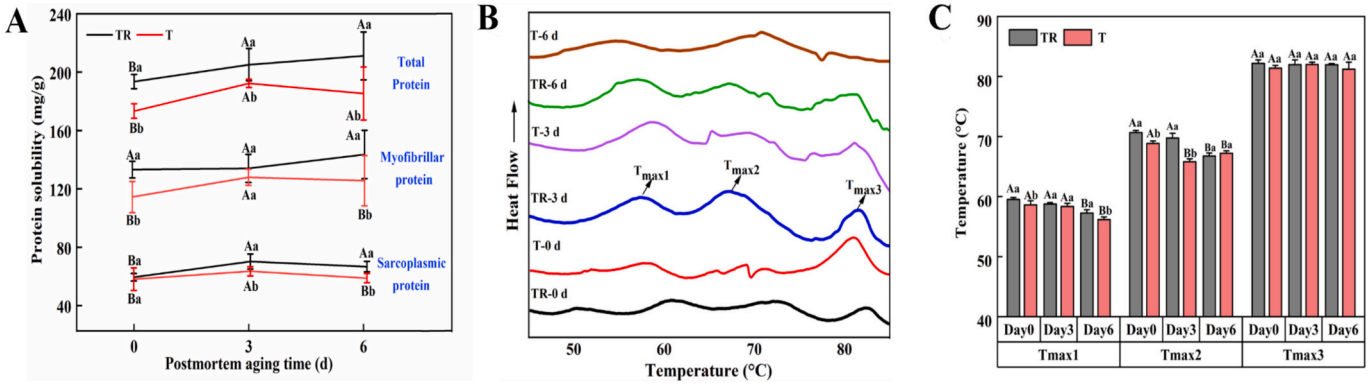

Fig. 5. Effects of pre-slaughter transport stress on the functional properties of pork protein during postmortem aging, (A) protein solubility, (B) DSC thermogram, and (C) maximum denaturation temperature (T_{max}). Different letters (A-C) indicate a significant difference among aging time points at the same treatment ($p < 0.05$); Different letters (a, b) indicate a significant difference between two treatments at the same aging time ($p < 0.05$). TR: three-hour transport followed by three-hour resting treatment; T: three-hour transport treatment.

covalent bonds within the protein molecule, and the breakage of intermolecular bonds (e.g., hydrogen bond) is responsible for the reduced T_{max} (Xie et al., 2021). Given the outcomes of the protein structure (Fig. 4), it was clear that the meat proteins of the T group showed a greater degree of unwinding and unfolding than those of the TR group during postmortem aging. Thus, relatively lower T_{max} values, including T_{max1} and T_{max2} in the T group, could be ascribed to the serious destruction of the regular structure of proteins.

3.5. Protein degradation

It has been widely accepted that the degradation of critical cytoskeleton proteins (such as desmin, TnT, and filamin C) regulated through several endogenous proteases is recognized as a fundamental factor affecting meat quality due to their direct and significant contribution to maintaining the structural integrity of myofibrils. Among several proteolytic enzymes, μ-calpain and caspase were found to be primarily responsible for postmortem proteolysis and have been a focus of attention for several decades (Du, Ma, Wang, Hao, & Zhang, 2023). Generally, the proteolytic activity of μ-calpain and caspase, especially caspase-3, is mainly derived from their degraded products, with higher degradation levels indicating stronger proteolytic activity. As shown in Fig. 6, the degradation levels of μ-calpain in T group were notably lower than those in TR group ($p < 0.05$), while no significant degraded difference was observed in caspase-3 ($p > 0.05$). However, for caspase-3 activity, it was found that T group showed a significantly lower degree ($p < 0.05$). These results indicated that T group muscles presented a lower proteolytic ability, which could be explained by higher oxidation levels during postmortem aging. As is known, μ-calpain and caspase-3 are a class of cysteine proteases with several active sites that are particularly sensitive to oxidative environments. Overproduction of ROS and RNS in postmortem muscle could directly exert an inhibitory role on μ-calpain degradation and caspase-3 activity via oxidation and S-nitrosylation modifications (Zhang et al., 2013). In addition, the degradation level of critical cytoskeleton proteins was also displayed in Fig. 6. Consistently, it is found that except for filamin C ($p > 0.05$), the degradation of desmin and TnT in T group had a significantly lower level relative to TR group ($p < 0.05$). In summary, these results demonstrate that T group muscle possessed impaired μ-calpain autolysis and caspase-3 activity, which was responsible for the reduced degradation of critical cytoskeleton proteins and thus for a higher structural integrity of myofibrils.

3.6. Microstructure

Morphological observation of muscle fibers is shown in Fig. 7A.

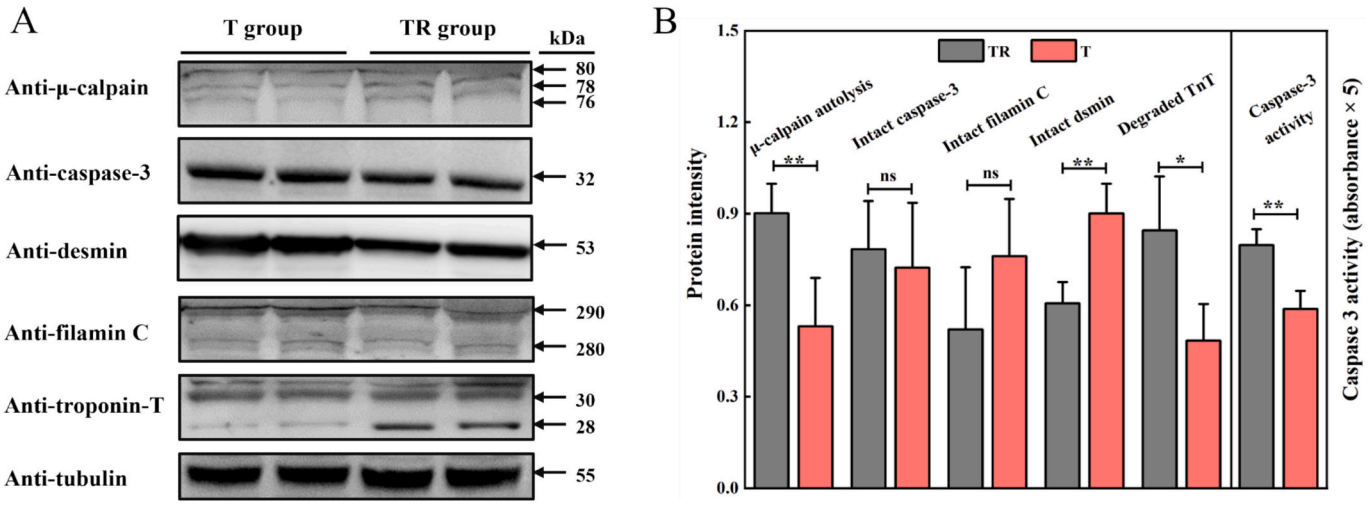

Fig. 6. Effects of pre-slaughter transport stress on the μ-calpain, caspase-3, and critical cytoskeleton proteins of pork LT muscle at 3 d of postmortem aging, (A) representative immunoblot bands and (B) intensity of target proteins and caspase-3 activity. "*" indicate a significant difference ($p < 0.05$), "**" indicate a significant difference ($p < 0.01$), and "ns" mean no significant difference. TR: three-hour transport followed by three-hour resting treatment; T: three-hour transport treatment.

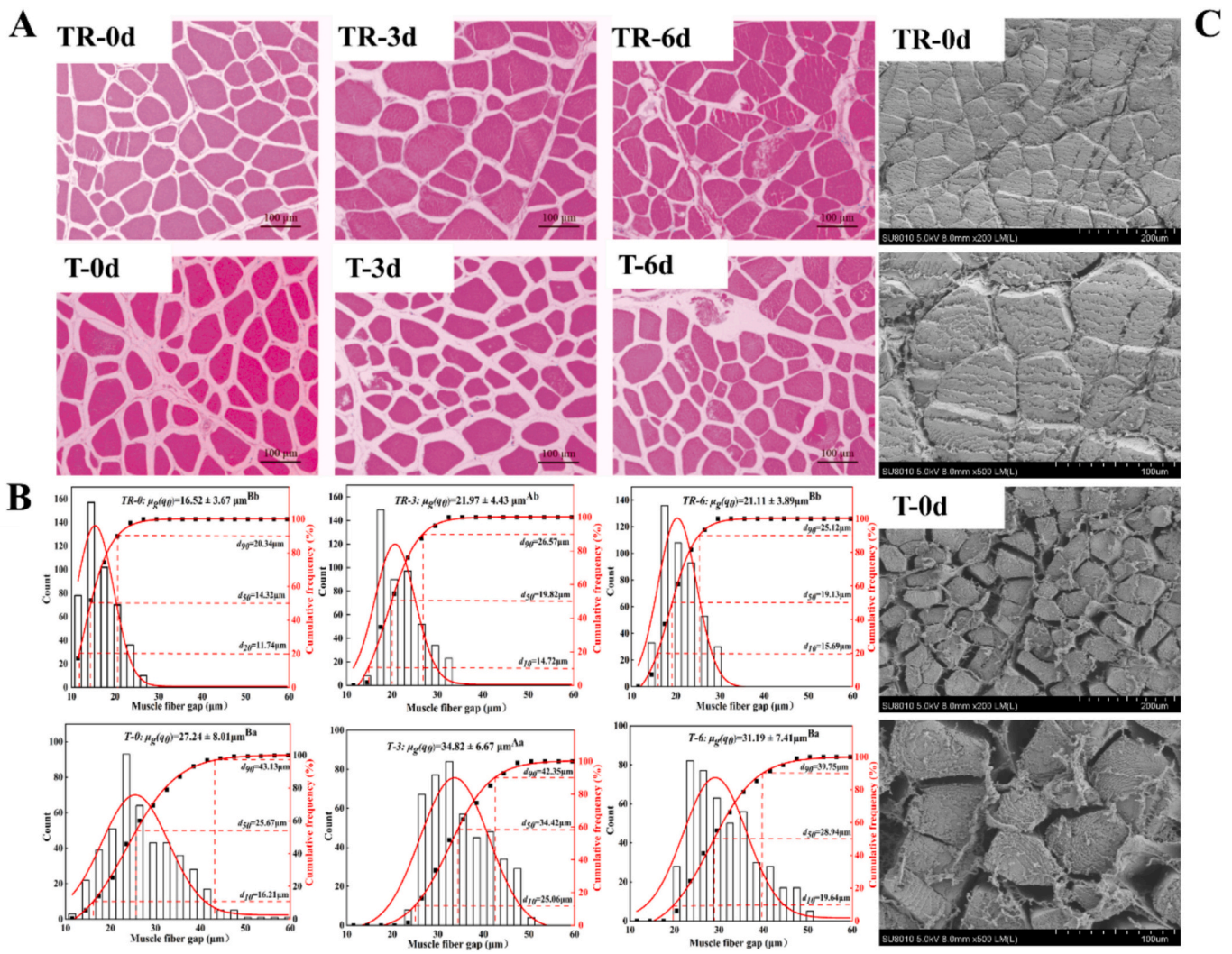

Fig. 7. Effects of pre-slaughter transport stress on the microstructure of pork LT muscle during postmortem aging, (A) representative H&E staining images, (B) average muscle fiber gap, and (C) representative SEM images. Different letters (A-C) indicate a significant difference among aging time points at the same treatment ($p < 0.05$); Different letters (a, b) indicate a significant difference between two treatments at the same aging time ($p < 0.05$). TR: three-hour transport followed by three-hour resting treatment; T: three-hour transport treatment.

During the aging of 6 d, muscle fiber structure of TR group was tightly aligned and filled in the endomysium. However, the T group was relatively loose and showed an atrophied shape. Besides, the size distribution of muscle fiber gap and cumulative frequency analysis indicates that the average muscle fiber gap in the T group was remarkably enlarged during whole aging compared with the TR group ($p < 0.05$, Fig. 7B). Taking 0 d as an example, the average muscle fiber gap in the TR group was 16.52 μm, with 90 % of the gaps <20.34 μm and 50 % < 14.32 μm. However, the average muscle fiber gap in the T group was 27.24 μm, with 90 % of the gaps <43.13 μm and 50 % < 25.67 μm. In addition, two groups of samples at 0 d were also used for SEM observation. As shown in Fig. 7C, the muscle fiber structure of the TR group was tightly and neatly arranged. In contrast, the muscle fiber bundles of the meat samples of the T group were clearly separated from each other, with severe contraction and obvious drip channel formation. A similar finding was reported by Xing, Xu, Zhang, and Gao (2022), who also observed a more intense muscle fiber contraction and a greater muscle fiber gap in broilers subjected to high-temperature transport stress. The intense muscle fiber contraction and the resulting increased muscle fiber gap were more likely to induce the formation of drip channels in the postmortem muscle (Hughes, Oiseth, Purslow, & Warner, 2014), which could further explain the impaired WHC of T group. Previously, Liu, Xiong, and Chen (2009) proposed one mechanism that oxidation could be involved in the regulation of meat WHC by structure alteration of myofibril which implicated the expanded muscle cell gap. As stated in the 3.5 section, the increased oxidation levels restricted the capacity of μ-calpain and caspase-3 to degrade their substrates such as desmin and TnT. When most cytoskeletal proteins remain more intact, myofibril contraction is readily transmitted to the entire myocyte inducing an increased muscle fiber gap and thereby a decreased WHC.

3.7. Connection between the changes in protein properties and impaired pork WHC in response to pre-slaughter transport stress

Fig. 8A and B represent the score and loading plots, respectively. Fig. 8A depicts the differences among the meat samples from pigs under different pre-slaughter stress levels during postmortem aging. At 3 and 6 d, the T and TR groups were obviously separated indicating remarkable WHC as well as protein-related indicator differences between the two groups. For the TR group, the 0 d samples were described by higher SH content and α-helix ratio, while the 3 and 6 d samples were characterized by higher protein solubility and P_{21}. For the T group, the 0 d samples were described by higher T_{21}, P_{22}, and particle size, while the 3 and 6 d samples were characterized by higher drip loss, cooking loss, T_{22},

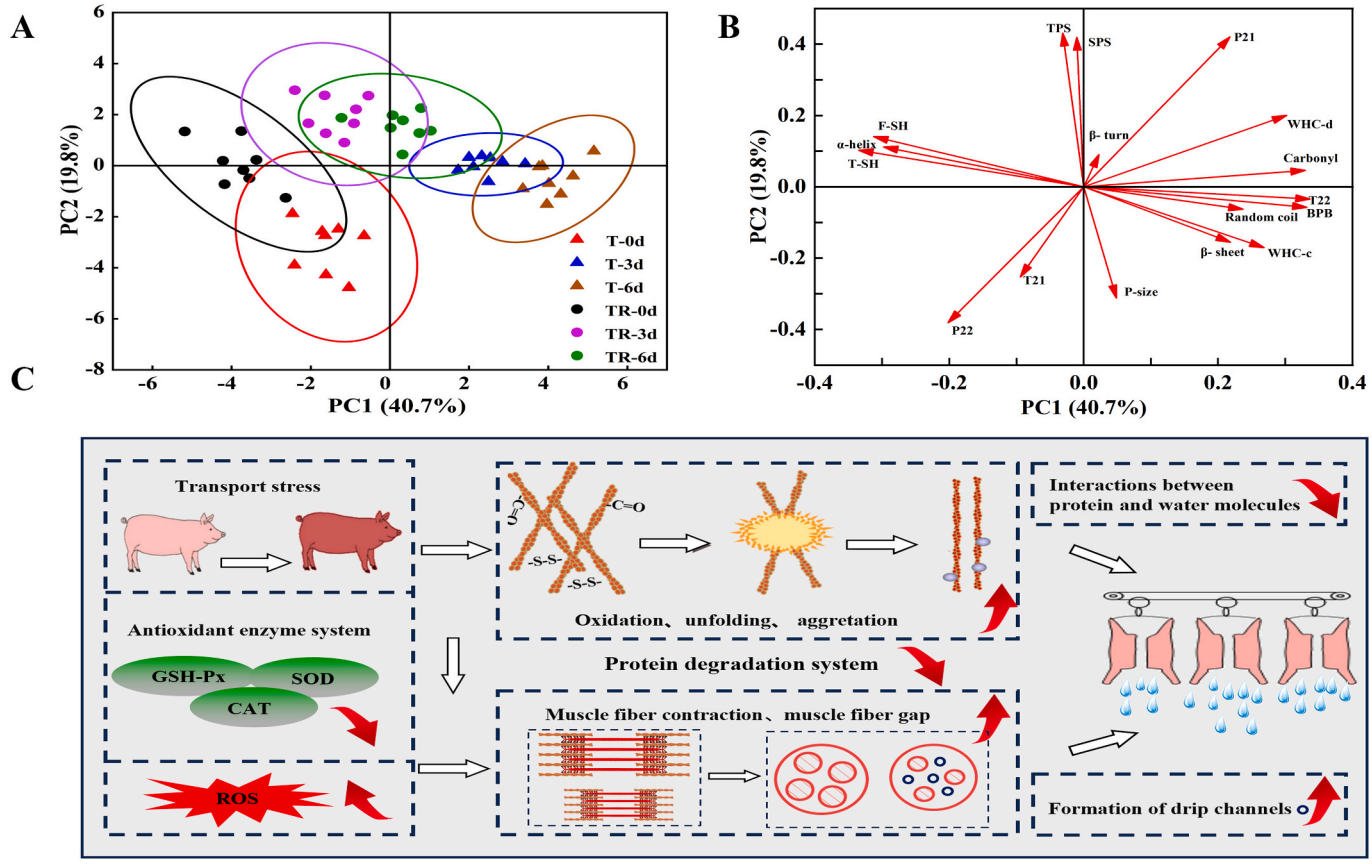

Fig. 8. PCA of the indicators of pork samples with different pre-slaughter handling methods and aging time as well as a schematic diagram of pre-slaughter transport stress impairing the water holding capacity of pork during postmortem aging, (A) loading plot, (B) scores plot, and (C) schematic diagram. TR: three-hour transport followed by three-hour resting treatment; T: three-hour transport treatment; WHC-d: drip loss; WHC-c: cooking loss; T-SH: total sulfhydryl; F-SH: free sulfhydryl; TPS: total protein solubility; SPS: sarcoplasmic protein solubility; BPB: surface hydrophobicity; P-size: particle size.

carbonyl content, surface hydrophobicity, β-sheet ratio, and random coil ratio.

Additionally, it can be observed from Fig. 8B that cooking loss, drip loss, and T_{22} showed negative correlations with SH content and α-helical ratio, however, positive correlations with carbonyl content, random coil ratio, surface hydrophobicity, and particle size. The results of the present study were similar to the previous studies demonstrating that meat WHC was negatively correlated with oxidation levels, solubility, and random coil ratio, however, positively correlated with α-helix structure and thermal stability (Estevez et al., 2011; Li et al., 2020). It has been reported that increased carbonyl groups as well as decreased SH groups and surface hydrophobicity were commonly accompanied by the formation of protein crosslinks (such as disulfide bonds and carbonyl-lysine Ɛ-amino crosslinks) (Feng, Yin, Zhou, Ma, & Zhang, 2023; Fu et al., 2019). As a result, the cohesive tightening effect of MP can be enhanced and thus limit the swelling of myofibrils reducing the ability of muscle fibers to retain water (Liu et al., 2009; Puolanne & Halonen, 2010). Besides, the formation of protein carbonyl and crosslinks is also involved in the loss of some charged amino acids, inducing a reduction in the net charge of the myofibrillar proteins (Utrera & Estévez, 2012). A relatively lower net charge means that there are fewer charged protein sites for binding water molecules and therefore may reduce the ability of muscle fibers to adsorb water (Bowker & Zhuang, 2015). On the other hand, in the current study, pre-slaughter transport stress exacerbated the degree of unwinding and unfolding of MP, inducing the exposure of many hydrophobic regions buried inside the protein and the damage of ordered α-helix structure. These alterations then could reduce the WHC of fresh meat during postmortem aging by weakening the binding capacity of protein and water molecules (Guo, Chen, Ma, Yu, & Zhang, 2023). Besides, numerous reports have indicated that protein denaturation levels were closely associated with the WHC of fresh meat. The denaturation of myosin could induce lateral contraction between muscle fibers, which could force moisture between muscle fibers to be expelled as juice loss (Pearce, Rosenvold, Andersen, & Hopkins, 2011). The denatured sarcoplasmic protein could precipitate on the surface of MP and shield the negative charges, thus decreasing the electrostatic repulsion between myofilaments. As a result, muscle proteins would further become tightly packed and in turn reduce the filament space, forcing immobilized water to migrate to free water and ultimately reducing WHC (Bowker & Zhuang, 2015).

4. Conclusions

This investigation found that transport-induced stress promoted water mobility and declined pork WHC during postmortem aging, which could be further verified by the increased muscle fiber gap. Meanwhile, transport stress led to higher oxidation levels of pork during postmortem aging. The results of protein secondary and tertiary structures indicate that transport-induced stress disrupted the regular spatial conformation of protein, causing a decreased α-helix ratio and an increased protein surface hydrophobicity. A notable increase in protein particle size as well as a remarkable decrease in solubility and thermal stability of proteins were also observed in transport stress group, indicating increased protein denaturation levels and impaired functional properties of protein. Additionally, the impaired μ-calpain autolysis and caspase-3 activity in T group led to reduced degradation of critical cytoskeleton proteins, which could be responsible for increased muscle contraction levels and thus the formation of drip channels. All in all, as

displayed in Fig. 8C, this study supports that the increased oxidation levels and varying physicochemical properties of proteins caused pre-slaughter transport stress could further reduce the muscle WHC via impairing the interactions between protein and water molecules as well as changing the structure of muscle fiber. However, this work only establishes a correlation between general oxidative parameters and pork quality, oxidation and carbonylation modifications in response to pre-slaughter stress are protein- and site-specific. Future research should further investigate the specific oxidized and carbonylated proteins mediating the effect of pre-slaughter stress on meat quality development by applying modification-specific proteomic analysis.

CRediT authorship contribution statement

Chao Ma: Writing – review & editing, Writing – original draft, Software, Methodology, Formal analysis, Data curation, Conceptualization. **Jian Zhang:** Writing – review & editing. **Ruyu Zhang:** Writing – review & editing. **Lei Zhou:** Writing – review & editing. **Laixue Ni:** Investigation. **Wangang Zhang:** Writing – review & editing, Supervision, Funding acquisition, Conceptualization.

Declaration of competing interest

The authors declare that they have no known competing financial interests or personal relationships that could have appeared to influence the work reported in this paper.

Data availability

Data will be made available on request.

Acknowledgments

This work was funded by the National Natural Science Foundation of China (32372358) and the Jiangsu Agricultural Science and Technology Innovation Fund (CX (23)3141).

Appendix A. Supplementary data

Supplementary data to this article can be found online at https://doi.org/10.1016/j.fochx.2024.101913.

References

Bowker, B., & Zhuang, H. (2015). Relationship between water-holding capacity and protein denaturation in broiler breast meat. *Poultry Science, 94*(7), 1657–1664. https://doi.org/10.3382/ps/pev120

Cao, M., Cao, A., Wang, J., Cai, L., Regenstein, J., Ruan, Y., & Li, X. (2018). Effect of magnetic nanoparticles plus microwave or far-infrared thawing on protein conformation changes and moisture migration of red seabream (*Pagrus Major*) fillets. *Food Chemistry, 266*, 498–507. https://doi.org/10.1016/j.foodchem.2018.06.057

Cao, Y. G., & Xiong, Y. L. L. (2015). Chlorogenic acid-mediated gel formation of oxidatively stressed myofibrillar protein. *Food Chemistry, 180*, 235–243. https://doi.org/10.1016/j.foodchem.2015.02.036

Carvalho, R. H., Ida, E. I., Madruga, M. S., Martinez, S. L., Shimokomaki, M., & M.. (2017). Underlying connections between the redox system imbalance, protein oxidation and impaired quality traits in pale, soft and exudative (PSE) poultry meat. *Food Chemistry, 215*, 129–137. https://doi.org/10.1016/j.foodchem.2016.07.182

Chelh, I., Gatellier, P., & Sante-Lhoutellier, V. (2006). Technical note: A simplified procedure for myofibril hydrophobicity determination. *Meat Science, 74*(4), 681–683. https://doi.org/10.1016/j.meatsci.2006.05.019

Chen, L., Zhou, G. H., & Zhang, W. G. (2015). Effects of high oxygen packaging on tenderness and water holding capacity of pork through protein oxidation. *Food and Bioprocess Technology, 8*(11), 2287–2297. https://doi.org/10.1007/s11947-015-1566-0

Cheng, S., He, Y., Zeng, T., Wang, D., He, J., Xia, Q., Zhou, C., Pan, D., & Cao, J. (2022). Heat stress induces various oxidative damages to myofibrillar proteins in ducks. *Food Chemistry, 390*, Article 133209. https://doi.org/10.1016/j.foodchem.2022.133209

Du, T., Ma, C., Wang, Z., Hao, Y., & Zhang, W. (2023). Distribution and degradation of pork filamin during postmortem aging. *Journal of Agricultural and Food Chemistry, 71*(41), 15287–15295. https://doi.org/10.1021/acs.jafc.3c04208

Du, X., Li, H. J., Nuerjiang, M., Rui, L. T., Kong, B. H., Xia, X. F., & Shao, M. L. (2021). Influence of repeated freeze-thaw treatments on the functional and structural properties of myofibrillar protein from mirror carp (*Cyprinus carpio* L.). *Food Biophysics, 16*(4), 492–501. https://doi.org/10.1007/s11483-021-09689-5

Estevez, M., Ventanas, S., Heinonen, M., & Puolanne, E. (2011). Protein carbonylation and water-holding capacity of pork subjected to frozen storage: Effect of muscle type, premincing, and packaging. *Journal of Agricultural and Food Chemistry, 59*(10), 5435–5443. https://doi.org/10.1021/jf104995j

Faucitano, L. (2018). Preslaughter handling practices and their effects on animal welfare and pork quality. *Journal of Animal Science, 96*(2), 728–738. https://doi.org/10.1093/jas/skx064

Feng, F., Yin, Y. T., Zhou, L., Ma, C., & Zhang, W. G. (2023). Effect of nitric oxide and its induced protein S-nitrosylation on the structures and in vitro digestion properties of beef myofibrillar protein. *Journal of Agricultural and Food Chemistry, 71*(5), 2532–2540. https://doi.org/10.1021/acs.jafc.2c07804

Fu, Q. Q., Liu, R., Wang, H. O., Hua, C., Song, S. X., Zhou, G. H., & Zhang, W. G. (2019). Effects of oxidation *in vitro* on structures and functions of myofibrillar protein from beef muscles. *Journal of Agricultural and Food Chemistry, 67*(20), 5866–5873. https://doi.org/10.1021/acs.jafc.9b01239

Guo, Z., Chen, C., Ma, G., Yu, Q., & Zhang, L. (2023). LF-NMR determination of water distribution and its relationship with protein- related properties of yak and cattle during postmortem aging. *Food Chemistry: X, 20*, Article 100891. https://doi.org/10.1016/j.fochx.2023.100891

Hughes, J. M., Oiseth, S. K., Purslow, P. P., & Warner, R. D. (2014). A structural approach to understanding the interactions between colour, water-holding capacity and tenderness. *Meat Science, 98*(3), 520–532. https://doi.org/10.1016/j.meatsci.2014.05.022

Jiang, S., Zhang, M., Liu, H., Li, Q., Xue, D. J., Nian, Y. Q., … Li, C. B. (2022). Ultrasound treatment can increase digestibility of myofibrillar protein of pork with modified atmosphere packaging. *Food Chemistry, 377*, 10. https://doi.org/10.1016/j.foodchem.2021.131811

Kang, D. C., Zou, Y. H., Cheng, Y. P., Xing, L. J., Zhou, G. H., & Zhang, W. G. (2016). Effects of power ultrasound on oxidation and structure of beef proteins during curing processing. *Ultrasonics Sonochemistry, 33*, 47–53. https://doi.org/10.1016/j.ultsonch.2016.04.024

Lesiów, T., & Xiong, Y. L. (2013). A simple, reliable and reproductive method to obtain experimental pale, soft and exudative (PSE) pork. *Meat Science, 93*(3), 489–494. https://doi.org/10.1016/j.meatsci.2012.11.022

Li, F., Zhong, Q., Kong, B., Wang, B., Pan, N., & Xia, X. (2020). Deterioration in quality of quick-frozen pork patties induced by changes in protein structure and lipid and protein oxidation during frozen storage. *Food Research International, 133*, Article 109142. https://doi.org/10.1016/j.foodres.2020.109142

Li, F. F., Wang, B., Kong, B. H., Shi, S., & Xia, X. F. (2019). Decreased gelling properties of protein in mirror carp (*Cyprinus carpio*) are due to protein aggregation and structure deterioration when subjected to freeze-thaw cycles. *Food Hydrocolloids, 97*, 8. https://doi.org/10.1016/j.foodhyd.2019.105223

Li, Q., Sun, X., Mubango, E., Zheng, Y., Liu, Y., Zhang, Y., … Hong, H. (2023). Effects of protein and lipid oxidation on the water holding capacity of different parts of bighead carp: Eye, dorsal, belly and tail muscles. *Food Chemistry, 136238*. https://doi.org/10.1016/j.foodchem.2023.136238

Liao, H., Zhang, L., Li, J., Xing, T., & Gao, F. (2022). Acute stress deteriorates breast meat quality of Ross 308 broiler chickens by inducing redox imbalance and mitochondrial dysfunction. *Journal of Animal Science, 100*(9). https://doi.org/10.1093/jas/skac221

Liu, Z. L., Xiong, Y. L. L., & Chen, J. (2009). Identification of restricting factors that inhibit swelling of oxidized myofibrils during brine irrigation. *Journal of Agricultural and Food Chemistry, 57*(22), 10999–11007. https://doi.org/10.1021/jf902722j

Ma, C., Zhang, W., Zhang, J., & Du, T. (2023). Modification-specific proteomic analysis reveals cysteine S-nitrosylation mediated the effect of preslaughter transport stress on pork quality development. *Journal of Agricultural and Food Chemistry, 71*(50), 20260–20273. https://doi.org/10.1021/acs.jafc.3c05254

Ma, C., Zhang, W., Zhou, L., & Feng, F. (2023). Effect of pre-slaughter transport stress on protein S-nitrosylation levels of pork during postmortem aging. *Journal of Agricultural and Food Chemistry, 71*(29), 11150–11157. https://doi.org/10.1021/acs.jafc.3c00907

Pearce, K. L., Rosenvold, K., Andersen, H. J., & Hopkins, D. L. (2011). Water distribution and mobility in meat during the conversion of muscle to meat and ageing and the impacts on fresh meat quality attributes - a review. *Meat Science, 89*(2), 111–124. https://doi.org/10.1016/j.meatsci.2011.04.007

Promeyrat, A., Gatellier, P., Lebret, B., Kajak-Siemaszko, K., Aubry, L., & Santé-Lhoutellier, V. (2010). Evaluation of protein aggregation in cooked meat. *Food Chemistry, 121*(2), 412–417. https://doi.org/10.1016/j.foodchem.2009.12.057

Puolanne, E., & Halonen, M. (2010). Theoretical aspects of water-holding in meat. *Meat Science, 86*(1), 151–165. https://doi.org/10.1016/j.meatsci.2010.04.038

Qiu, S., Cui, F. C., Wang, J. X., Zhu, W. H., Xu, Y. X., Yi, S. M., … Li, J. R. (2022). Effects of ultrasound-assisted immersion freezing on the muscle quality and myofibrillar protein oxidation and denaturation in *Sciaenops ocellatus*. *Food Chemistry, 377*, 9. https://doi.org/10.1016/j.foodchem.2021.131949

Salas, R. C. D., & Mingala, C. N. (2017). Genetic factors affecting pork quality: Halothane and rendement napole genes. *Animal Biotechnology, 28*(2), 148–155. https://doi.org/10.1080/10495398.2016.1243550

Shelepov, V., Tihonov, S., Gorlov, I., & Poznyakovskiy, V. (2015). About the quality of meat with PSE and DFD properties. *Foods and Raw Materials, 3*(1), 104–110. https://doi.org/10.12737/11244

Szmanko, T., Lesiow, T., & Gorecka, J. (2021). The water-holding capacity of meat: A reference analytical method. *Food Chemistry, 357*, 6. https://doi.org/10.1016/j.foodchem.2021.129727

Utrera, M., & Estévez, M. (2012). Oxidation of myofibrillar proteins and impaired functionality: Underlying mechanisms of the carbonylation pathway. *Journal of Agricultural and Food Chemistry, 60*(32), 8002–8011. https://doi.org/10.1021/jf302111j

Wang, C., Wang, H., Li, X., & Zhang, C. H. (2019). Effects of oxygen concentration in modified atmosphere packaging on water holding capacity of pork steaks. *Meat Science, 148*, 189–197. https://doi.org/10.1016/j.meatsci.2018.10.001

Xie, Y., Chen, B., Guo, J., Nie, W., Zhou, H., Li, P., Zhou, K., & Xu, B. (2021). Effects of low voltage electrostatic field on the microstructural damage and protein structural changes in prepared beef steak during the freezing process. *Meat Science, 179*, Article 108527. https://doi.org/10.1016/j.meatsci.2021.108527

Xing, T., Gao, F., Tume, R. K., Zhou, G. H., & Xu, X. L. (2019). Stress effects on meat quality: A mechanistic perspective. *Comprehensive Reviews in Food Science and Food Safety, 18*(2), 380–401. https://doi.org/10.1111/1541-4337.12417

Xing, T., Li, Y. H., Li, M., Jiang, N. N., Xu, X. L., & Zhou, G. H. (2016). Influence of transport conditions and pre-slaughter water shower spray during summer on protein characteristics and water distribution of broiler breast meat. *Animal Science Journal, 87*(11), 1413–1420. https://doi.org/10.1111/asj.12593

Xing, T., Xu, X. L., Zhang, L., & Gao, F. (2022). Overexpression of heat shock protein 70 ameliorates meat quality of broilers subjected to pre-slaughter transport at high ambient temperatures by improving energy status of pectoralis major muscle and antioxidant capacity. *Antioxidants, 11*(8), 13. https://doi.org/10.3390/antiox11081468

Yin, Y., Zhou, L., Pereira, J., Zhang, J., & Zhang, W. (2020). Insights into digestibility and peptide profiling of beef muscle proteins with different cooking methods. *Journal of Agricultural and Food Chemistry, 68*(48), 14243–14251. https://doi.org/10.1021/acs.jafc.0c04054

Yin, Y. T., Xing, L., & Zhang, W. (2023). Moderate protein oxidation improves bovine myofibril digestibility by releasing peptides in the S2 region of myosin: A peptidomics perspective. *Journal of Agricultural and Food Chemistry, 71*(5), 2514–2522. https://doi.org/10.1021/acs.jafc.2c07708

Young, J. F., Bertram, H. C., & Oksbjerg, N. (2009). Rest before slaughter ameliorates pre-slaughter stress-induced increased drip loss but not stress-induced increase in the toughness of pork. *Meat Science, 83*(4), 634–641. https://doi.org/10.1016/j.meatsci.2009.07.019

Zhang, W. G., Xiao, S., & Ahn, D. U. (2013). Protein oxidation: Basic principles and implications for meat quality. *Critical Reviews in Food Science and Nutrition, 53*(11), 1191–1201. https://doi.org/10.1080/10408398.2011.577540

Zhang, Y., Li, Y., Guo, J., Feng, Y., Xie, Q., Guo, M., Yin, J., & Liu, G. (2024). Effect of two-stage low-temperature tempering process assisted by electrostatic field application on physicochemical and structural properties of myofibrillar protein in frozen longissimus dorsi of tan mutton. *Food Chemistry, 456*, Article 140001. https://doi.org/10.1016/j.foodchem.2024.140001

Zhou, B., Shen, Z. L., Liu, Y. S., Wang, C. T., & Shen, Q. W. W. (2019). Proteomic analysis reveals that lysine acetylation mediates the effect of antemortem stress on postmortem meat quality development. *Food Chemistry, 293*, 396–407. https://doi.org/10.1016/j.foodchem.2019.04.122